

AVEIRO - PORTUGAL



This paper must be cited as:

Moura, R.T., Carneiro Neto, A.N., Aguiar, E.C., Santos, C.V., de Lima, E.M., Faustino, W.M., Teotonio, E.E.S., Brito, H.F., Felinto, M.C.F.C., Ferreira, R.A.S., Carlos, L.D., Longo, R.L., Malta, O.L., Optical Materials: X. 11, 2021, 100080, <https://doi.org/10.1016/j.omx.2021.100080>

JOYSpectra: a web platform for luminescence of lanthanides

Renaldo T. Moura Jr.,^{1*} Albano N. Carneiro Neto,^{2*} Eduardo C. Aguiar,³ Carlos V. Santos-Jr.,⁴ Ewerton M. de Lima,¹ Wagner M. Faustino,⁵ Ercules E. S. Teotonio,⁵ Hermi F. de Brito,⁶ Maria C.F.C. Felinto,⁷ Rute A. S. Ferreira,² Luís D. Carlos,² Ricardo L. Longo,⁸ and Oscar L. Malta,^{8*}

Correspondence to: Renaldo T. Moura Jr. (email: renaldo.mourajr@cca.ufpb.br); Albano N. Carneiro Neto (email: albanoneto@ua.pt); and Oscar L. Malta (email: oscar.malta@ufpe.br)

¹ Department of Chemistry and Physics, Federal University of Paraíba, Areia-PB, 58397-000, Brazil

² Physics Department and CICECO – Aveiro Institute of Materials, University of Aveiro, Aveiro, 3810-193, Portugal

³ Academic Unity of Belo Jardim, Federal Rural University of Pernambuco, Belo Jardim-PE, 55156-580, Brazil

⁴ Department of Chemistry, Federal University of Rio Grande do Norte, Natal-RN, 59078-970, Brazil

⁵ Department of Chemistry, Federal University of Paraíba, João Pessoa-PB, 58051-970, Brazil

⁶ Institute of Chemistry, University of São Paulo, São Paulo-SP, 05508-000, Brazil

⁷ Nuclear and Energy Research Institute - IPEN/CNEN, São Paulo-SP, 05508-000, Brazil

⁸ Department of Fundamental Chemistry, Federal University of Pernambuco, Recife-PE, 50670-901, Brazil

Abstract

JOYSpectra is a free-of-charge web platform for perform online calculations of spectroscopic properties of lanthanide-based compounds and materials. It has several features and functionalities to provide a detailed analysis of the intensity parameters. For instance, their dependence with the chemical environment of the lanthanide ion such as structure and nature of ligating atoms, can be performed automatically and take into account covalency and thermal effects. The program can also calculate the intramolecular energy transfer rates from a single donor state (S_1 or T_1) up to 310 transitions involving 12 Ln^{3+} ions. The web platform was designed to be user-friendly for experimentalists and theoreticians interested in calculations and analysis of the photophysical behavior of lanthanides. Its use requires only the structure of the compound and the choices of a few calculation options. To show its easiness and usefulness, a detailed step-by-step calculation and analysis are performed for the $[\text{Ln}(\text{tta})_3(\text{H}_2\text{O})_2]$ (Ln : Eu^{3+} and Tb^{3+}) complexes to explain and quantify their distinct luminescence.

Keywords:

Lanthanide spectroscopy; web platform; JOYSpectra; 4f-4f intensities; intramolecular energy transfer

1. Introduction

Lanthanide-based¹ compounds and materials have a wide range of applications, including commercial ones, where several of those are related to the unique photophysical and optical properties of lanthanide ions [1–10]. To achieve such a success and to continue striving towards further developments and breakthroughs the careful determination, categorization, and rationalization as well as theoretical/computational descriptions of their properties were and are paramount. In this context, the contributions in the

¹ For historical reasons we are not employing the recommended IUPAC name lanthanoid.

experimental front and theoretical interpretations made by professor G. Blasse, his students and collaborators cannot be overstressed [11–16]. His and many other research groups have applied, extended, and advanced the most successful theory for describing the luminescence of lanthanide ions, namely, the Judd-Ofelt theory [17,18,27–30,19–26]. This theory [17,18] and its improvements [31,32,41,33–40] have been used to rationalize and even predict most photophysical and luminescent properties of lanthanide-based compounds and materials, especially, 4f-4f transition intensities, radiative and non-radiative intramolecular energy transfer (IET) (ligand-lanthanide ion and ion-ion) processes [28,30,32,42–45].

In conjunction with their unique optical properties, the structural and electronic diversity of lanthanide-based compounds can be explored and applied in designing new functional materials such as molecular logic devices [46], UV dosimeters [47], luminescent nanothermometers [48], persistent luminescent phosphors [49–51], and other optical-magnetic technologies [52,53]. The comprehension and use of these properties of lanthanide ions depend on their electronic and molecular structures in solution and solid-state. In this context, computational chemistry methods are important and complementary tools to experiments. There are few computational programs developed for lanthanide-based compounds and for modeling their spectroscopic properties, namely, LUMPAC, JOES, and RELIC.

The LUMPAC program, developed by Dutra *et al.* [54], has been designed to be a user-friendly program for Windows® operating systems. It is divided into four modules ranging from geometry optimization to emission quantum yield estimates for Tb³⁺ and Eu³⁺ compounds. Geometry optimization is based on sparkle/semiempirical methods [55] within the MOPAC program [56]. The theoretical intensity parameters Ω_λ are calculated based on the expressions of the Simple Overlap Model (SOM) for the odd-component of the ligand field [34,35] and the dynamic coupling (DC) mechanism for the ligand-polarizability contributions [57]. The latter does not take into consideration the covalency effect as considered explicitly in the Bond Overlap Model (BOM) [33].

The JOES program, developed by Ćirić *et al.* [58], was recently released to calculate the intensity parameters Ω_λ from experimental emission spectra of Eu³⁺ compounds. The program has a large database of refractive indexes, n , for *ca.* 140 inorganic materials, which is important to obtain the magnetic allowed spontaneous emission coefficient for the ⁵D₀ → ⁷F₁ transition (A_{0→1}), because it depends on the third power of n . The value of A_{0→1} is used as an internal reference for the calculations of the Ω_λ from emission spectra of Eu³⁺ systems. Hence, any difference in n may lead to errors in the Ω_λ as well as in the total radiative emission coefficients (A_{rad}) and, consequently, the overall quantum yield [59].

The RELIC (Rare Earth Level and Intensity Calculations) program was developed by Hehlen *et al.* [31] and allows the user to calculate intermediate-coupling wavefunctions, energy levels, transition strengths, and radiative decay properties of Ln³⁺ (from Pr³⁺ to Tm³⁺) ions in solids. Unfortunately, the program is no longer available due to maintenance discontinuation, presenting some incompatibilities with each new version of the Windows operating system [60].

In the present work, we introduce a new web platform, named JOYSpectra, for calculating the luminescent properties of Ln-based materials. The platform was developed as a website on which the user can submit the input data for calculating the desired property (*e.g.*, intensity parameters Ω_λ , IET rates). The calculations are performed in a dedicated queue system composed of two computers and at the conclusion of the requested calculation, the user will receive the output data by email.

The JOYSpectra intends to be useful for both theoreticians and experimentalists in the field of lanthanide luminescence. Furthermore, it is free-of-charge and has relevant features that allow a better understanding of the chemical and physical information underlying the Ω_λ and IET quantities. This has relevance not only on for 4f-4f intensities, concerning covalency effects but also for IET processes in which, whenever necessary, only the forced-electric dipole (FED) mechanism contributing to the Ω_λ parameters should be considered.

The immediate advantages of the platform are:

1. The platform, as a website, is always updated.
2. The user does not need to perform an installation procedure of the program, thus avoiding problems such as operating system compatibility.
3. The calculations include covalency effects in Ω_λ , mainly in the dynamic coupling mechanism (DC) through the overlap polarizability α_{OP} [33].
4. The program can calculate IET rates from a single donor state (S_1 or T_1) up to Ln^{3+} 310 transitions, namely, Pr^{3+} 12, Nd^{3+} 20, Pm^{3+} 29, Sm^{3+} 34, Eu^{3+} 40, Gd^{3+} 13, Tb^{3+} 78, Dy^{3+} 21, Ho^{3+} 35, Er^{3+} 15, Tm^{3+} 12, and Yb^{3+} 1 transitions.
5. The user can set the temperature to calculate the forward and backward IET rates, considering an exponential-type the energy mismatch condition depending on which are the donor and the acceptor states.

We intend to present a brief description of the JOYSpectra web platform, detailing its features. In addition, we provide illustrative examples of the use of JOYSpectra for the complexes $[Ln(tta)_3(H_2O)_2]$ (Ln : Eu^{3+} and Tb^{3+} ; tta^- : thenoyltrifluoroacetate). These systems are known in the literature [61–63] due to their distinct IET behavior, where luminescence quenching is observed only in the Tb^{3+} complex, despite of both compounds being isostructural.

2. JOYSpectra web platform

The JOYSpectra was developed using a variety of computational languages (C/C++, PHP, HTML, Python, and Unix-based Shellscript) and its structure can be divided into front-end and back-end modules. Figure 1 shows a flowchart that schematizes the JOYSpectra web platform. The front-end is constituted of PHP/HTML codes and the inclusion of the JSmol [64] (an interactive web browser object) for structure visualization. The front-end is the user-friendly interface that allows the easy usage of the JOYSpectra. The back-end is written in C/C++, Python, and Unix-based Shellscript, and is the module that runs all the calculations available in the web platform. Each part of the online application presented in Figure 1 can be detailed as follows:

- a. Input.** The first, and mandatory, data that must be provided is the geometry of the compound. The JOYSpectra web platform is capable to read geometry coordinates from Gaussian [65], Orca [66], and MOPAC [56] output file formats. Also, the Cartesian coordinates (x, y, z) can be included directly in the online form. Crystallographic Information File (CIF) is not readable directly by the JOYSpectra, which requires a cif-file manipulation for the structural model extraction.
- b. User-friendly interface.** Once the geometry of the compound is provided, it is possible to proceed to the main web platform window. In this step, the web platform allows the choice of different options, each requiring specific input data. General data can be defined, and some functionalities will depend on the user's choice. Each option can be handled as follows:
 - b1. The intensity parameters Ω_λ and A_{rad}** are calculated as described in the Supplementary Information file (see subsections 1.1 and 1.2).

b1.1. The Judd-Ofelt intensity parameters can be calculated in JOYSpectra in two different ways. The first one is by fitting g and α' values. This procedure requires, as input data, the values of Ω_λ obtained from experimental spectra. This is the most time-consuming module of JOYSpectra and is performed by parallel computation using OpenMP multithreading. It is important to emphasize that even having the experimental Ω_λ values, the theoretical counterparts are mandatory for the upcoming steps in IET rates calculation.

b1.2 and b1.3. The other manner for obtaining the Judd-Ofelt intensity parameters is by providing the SOM model [34,35] charge factors g and BOM [33,67] ligand effective polarizabilities α' for each Ln–L chemical bond in the compound.

b1.4. The JOYSpectra application allows, optionally, automated geometry manipulation of the atoms in the first coordination sphere, producing a profile of theoretical Ω_λ values as a function of geometries [68–70]. This is done by the R_{VAR} , θ_{VAR} , and ϕ_{VAR} functionalities, as well as the number and sizes of the steps.

b1.5. All the geometries manipulated by the JOYSpectra application have their first sphere geometries symmetry point group recognized. This information may be useful for the interpretation of calculated data.

b1.6. The JOYSpectra application can also consider the thermal effects on the positions of the ligating atoms directly bonded to the lanthanide [71]. This is performed by a Bose-Einstein distribution [72] and yields thermally averaged values: $\bar{\Omega}_\lambda$, $\bar{\Omega}_\lambda^{FED}$, and $\bar{\Omega}_\lambda^{DC}$. This is optional, and if chosen, it requires the number of configurations to be used in the calculation of geometric dispersions. Typical values are close to 10^6 random configurations around the equilibrium structure. The temperature is also required, and its default value is set at 298.15 K.

b2. The intramolecular energy transfer W and W_b rates are calculated using Eq. S15 –S17 described in the Supplementary Information. It is worth to mention that the form of the spectral overlap (Eq. S16) has been discussed in detail in several references [32,73–75].

b2.1. The IET rates in JOYSpectra are calculated for up to 310 transitions, from a single donor state (S_1 or T_1) to Ln³⁺ states, namely, Pr³⁺ 12, Nd³⁺ 20, Pm³⁺ 29, Sm³⁺ 34, Eu³⁺ 40, Gd³⁺ 13, Tb³⁺ 78, Dy³⁺ 21, Ho³⁺ 35, Er³⁺ 15, Tm³⁺ 12, and Yb³⁺ 1 transitions.

b2.1. Temperature effects are accounted for in the IET rates by an exponential-type energy mismatch factor [32]. Also, if the option described in **b1.6** is chosen to be applied, the thermally averaged $\bar{\Omega}_\lambda^{FED}$ [72] will be used in IET rates calculation instead of the single value Ω_λ^{FED} of the equilibrium structure (considering only Eq. S3).

b3. Options soon to be available. These are the upcoming implementations that will soon be available in the JOYSpectra web platform and all of them have already been used in prior publications. The rate equations [32,59,76] are widely used to connect the microscopic rates with experimental photophysical data and their numerical solutions can provide theoretical emission quantum yields [77–79] and lifetimes [80]. Also, Ln³⁺ to Ln³⁺ energy transfer rates [44,45,72,81] and metallic nanoparticles plasmon effects [82,83] are recently explored in the literature.

c. Online calculation. After the choice of all options and functionalities described in **b**, it is possible to submit the calculation to be executed on the online server. Also, it is possible to follow the calculation queue status.

- d. Results sent by email.** When the online calculation is finished, the results are sent by the registered user email and then automatically deleted from our server. The email forwards the input and output files, that can be read in the JOYSpectra web platform.
- e. Output viewer.** The output file received by the user by email can be viewed in the JOYSpectra web platform. The functionality will print out the molecular geometry used to run the calculation. A summary of experimental and theoretical Ω_λ (with $\Omega_\lambda^{\text{FED}}$ and $\Omega_\lambda^{\text{DC}}$ contributions) will be displayed. If the IET rates calculation has been requested, a Jablonski-type diagram will be generated with the results, in addition to detailed information of all mechanisms calculated for all transitions considered. Also, all Ln–ligating atom chemical bond properties are shown. These and other information are presented in the output file.
- f. All these functionalities** are available through the QR code or link described in [Figure 1f](#). The interface for external users was constructed in PHP language and can be accessed through <http://slater.cca.ufpb.br/joyspectra>. A simple registration is required to use the platform and to access the computer facilities.

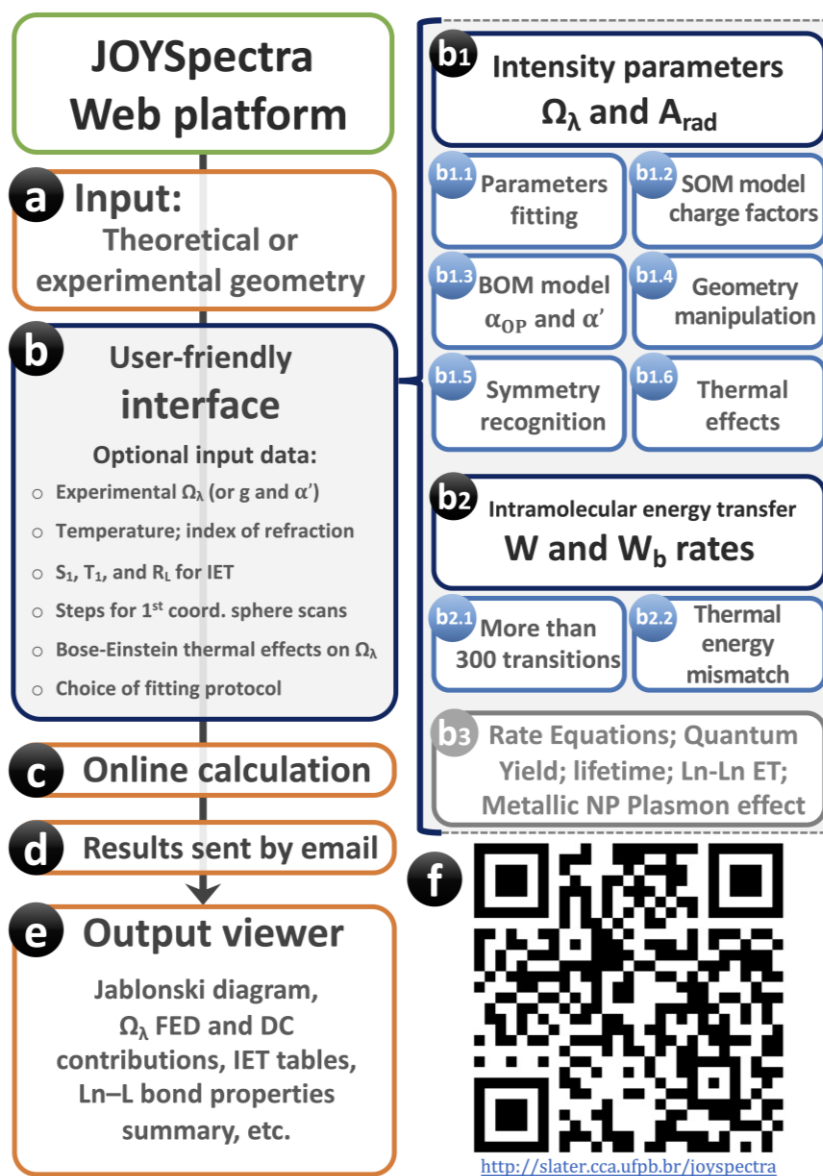


Figure 1. General scheme of the JOYSpectra web platform showing the main steps and functionalities. Also, the QR code and website are shown. Sugiuro modifcar: “Thermal effects accounted” para “Thermal effects” e “Thermal energy barrier” para “Thermal energy mismatch”; incluir “Lifetime” em b3

3. Illustrative example

Here we present a step-by-step example of the use of the JOYSpectra web platform for the $[\text{Ln}(\text{tta})_3(\text{H}_2\text{O})_2]$ (Ln: Eu^{3+} and Tb^{3+} ; tta^- : thenoyltrifluoroacetate) coordination compounds. These systems are an interesting example, due to their differences in photoluminescence properties. The compound with Eu^{3+} presents a reasonable red emission [63], while the Tb^{3+} counterpart exhibits a strong luminescence quenching [62]. Here, it will be shown the application of JOYSpectra to elucidate this experimental observation, illustrating its prediction capability for the IET behavior with the tta^- ligand acting as a good sensitizer for the Eu^{3+} and as a quencher for the Tb^{3+} compound.

A good starting point for a recommended use of JOYSpectra is inspecting the structural features of the compounds, noticing that $[\text{Eu}(\text{tta})_3(\text{H}_2\text{O})_2]$ and $[\text{Tb}(\text{tta})_3(\text{H}_2\text{O})_2]$ are isostructural. The geometry illustrated in Figure 2a was extracted from Ref. [84] (CCDC code: 758487 for Eu^{3+} compound) and shows a coordinatin number 8 with non-equivalent ligands. From a ligand field point of view, the relevant feature

is the ligating atoms, so we can consider all three tta^- ligands equivalents. However, the tta^- ligand is asymmetric $[\text{R}^1\text{-C(O)-CH-C(O)-R}^2]^-$ with substituents $\text{R}^1 = \text{CF}_3$ and $\text{R}^2 = \text{C}_4\text{H}_3\text{S}$ having very distinct character, which leads to ligating oxygen atoms with different electron densities. Therefore, a possible model for describing the coordination polyhedron consists of three equivalent oxygen atoms, denoted as FIT1, adjacent to the $-\text{CF}_3$ group, another three equivalent oxygen atoms, denoted as FIT2, adjacent to the $-\text{C}_4\text{H}_3\text{S}$ group, all in the tta^- ligands, and two oxygen atoms, denoted as FIT3 and FIT4, in the H_2O ligands, as depicted in Figure 2b. These three sets of ligating oxygen atoms are then employed in the fitting protocol of steps **b1.1**, **b1.2**, and **b1.3** depicted in Figure 1.

Once the ligating atoms and the coordination polyhedron are defined, to calculate the IET rates it is mandatory to provide the excited states information, namely: the first singlet (S_1) and triplet (T_1) ligands excited states, the R_L values for each excited state, as well as their corresponding bandwidths, γ . It is important to emphasize that, in the calculations of the IET rates, both zero-phonon lines or energy barycenters of the S_1 and T_1 states on the ligands have been used in the literature. This choice will undoubtedly affect the energy mismatch conditions between donor and acceptor and, consequently, the IET rate values. A discussion on this issue may be found in Ref. [32]. In our example systems, given that the compounds are isostructural, it is reasonable to consider the same S_1 , T_1 , and their respective R_L and γ values for $[\text{Eu}(\text{tta})_3(\text{H}_2\text{O})_2]$ and $[\text{Tb}(\text{tta})_3(\text{H}_2\text{O})_2]$. Namely, $\text{S}_1 = 29900 \text{ cm}^{-1}$, $\text{T}_1 = 20300 \text{ cm}^{-1}$ (considering the zero-phonon line), and $\gamma = 3000 \text{ cm}^{-1}$ [61,63]. The donor-acceptor distance $R_L = 4.5 \text{ \AA}$ (for both S_1 and T_1) was taken from Ref. [62].

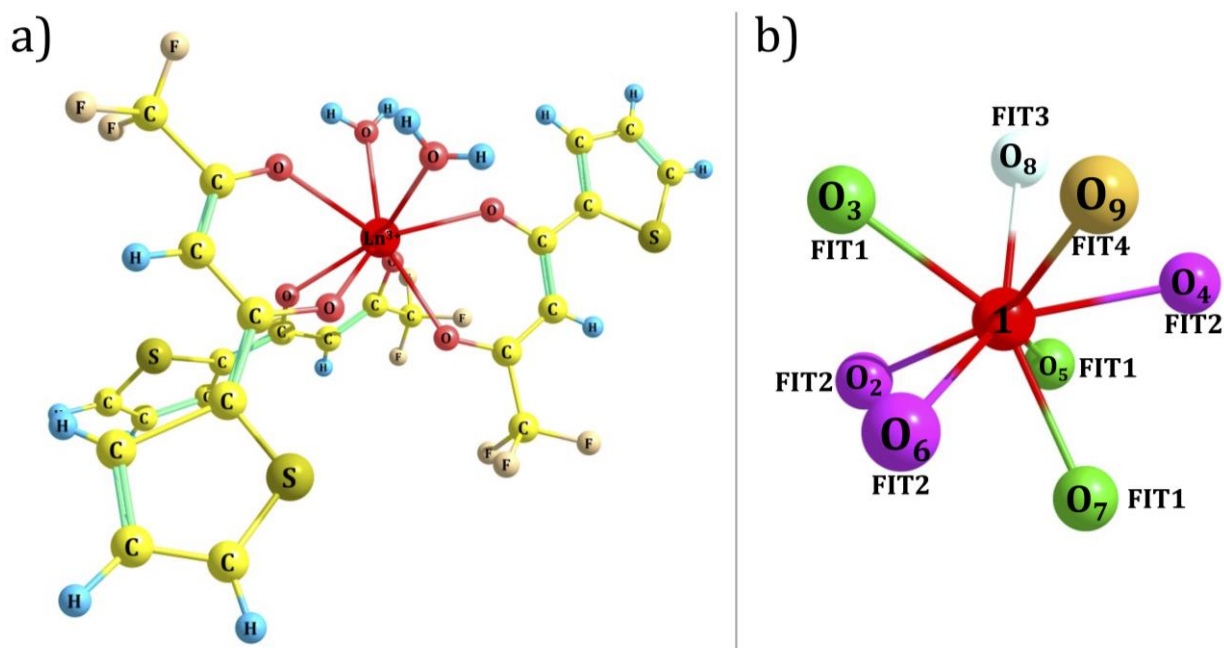


Figure 2. a) Structure of the $[\text{Ln}(\text{tta})_3(\text{H}_2\text{O})_2]$ (Ln : Eu^{3+} and Tb^{3+}). The geometry was extracted from the crystal structure data in Ref. [84] (CCDC code: 758487). The cartesian coordinates of this structure are in the Supplementary Information. b) Coordination polyhedron structure. Each color represents an oxygen atom with an equivalent chemical environment. The numbered oxygen labels correspond to the same ones shown in Table 1.

The JOYSpectra input files (Eu_tta.joy and Tb_tta.joy) created with this information for $[\text{Ln}(\text{tta})_3(\text{H}_2\text{O})_2]$ (Ln : Eu^{3+} and Tb^{3+}) can be found, as examples, at the web platform and in the Supplementary Information.

Using these files and running the JOYSpectra online calculation, the requested theoretical Ω_λ (with $\Omega_\lambda^{\text{FED}}$ and $\Omega_\lambda^{\text{DC}}$ contributions), IET rates (40 transitions for Eu^{3+} and 78 transitions for Tb^{3+}), and Ln–ligating atom

chemical bond properties (*i.e.*, fitted g and α' , and α_{OP} values) are obtained. [Tables 1](#) and [2](#) summarize these results, and the online output viewer assists their interpretation by building, among other things, the Jablonski-type diagrams as illustrated in [Figure 3](#). It is important to emphasize that the fitted g and α' values obtained for $[\text{Eu}(\text{tta})_3(\text{H}_2\text{O})_2]$ compound were used in $[\text{Tb}(\text{tta})_3(\text{H}_2\text{O})_2]$ calculations, because they are isostructural. This procedure was already performed in previous works [\[32,85\]](#).

Table 1. Values of α' (in \AA^3), α_{OP} (in 10^{-3}\AA^3), g (dimensionless), ρ (dimensionless), and R (in \AA) used for the calculation of the theoretical Ω_λ (in 10^{-20} cm^2) for $[\text{Eu}(\text{tta})_3(\text{H}_2\text{O})_2]$ complex. The FED contributions (those important for the energy transfer rates for the dipole-dipole mechanism) values are in parentheses. The experimental values of Ω_λ are $\Omega_2 = 33.0 \times 10^{-20} \text{ cm}^2$ and $\Omega_4 = 4.6 \times 10^{-20} \text{ cm}^2$ [\[86\]](#).

Ligating atom	Ligand type	α'	α_{OP}	g	ρ	R
O₂	tta ⁻	0.28	4.21	0.33	0.071	2.32
O₃	tta ⁻	0.24	3.85	0.32	0.066	2.37
O₄	tta ⁻	0.28	3.68	0.33	0.063	2.40
O₅	tta ⁻	0.24	3.58	0.32	0.062	2.41
O₆	tta ⁻	0.28	3.79	0.33	0.065	2.38
O₇	tta ⁻	0.24	3.93	0.32	0.067	2.36
O₈	H ₂ O	2.62	3.55	0.69	0.062	2.42
O₉	H ₂ O	3.20	3.66	0.72	0.063	2.40
[Eu(tta)₃(H₂O)₂]		Ω_2 (Ω_2^{FED})			33.05 (0.08)	
		Ω_4 (Ω_4^{FED})			8.17 (0.08)	
		Ω_6 (Ω_6^{FED})			1.45 (0.16)	

It can be observed in [Table 1](#) that the theoretical Ω_λ do not necessarily exactly match the experimental values, for Ω_4 in this case. As it will be shown, given that g and α' were fitted and yielded reasonable values for Ω_λ , the calculated $\Omega_\lambda^{\text{FED}}$ should also be reasonable to be used in IET rates calculation. In [Table 1](#), the observed charge factors g , ligand effective polarizability α' , and overlap polarizabilities, in ranges of $[0.32 - 0.78]$, $[0.24 - 3.2] \text{\AA}^3$, and $[3.55 - 4.21] \times 10^{-3} \text{\AA}^3$ respectively, are similar to those obtained for other β -diketonate ligands [\[69,70\]](#). The calculated values for the Tb^{3+} compound were $\Omega_2 = 26.23 \times 10^{-20} \text{ cm}^2$, $\Omega_4 = 6.08 \times 10^{-20} \text{ cm}^2$, and $\Omega_6 = 0.90 \times 10^{-20} \text{ cm}^2$, with the FED contributions: $\Omega_2^{\text{FED}} = 0.05 \times 10^{-20} \text{ cm}^2$, $\Omega_4^{\text{FED}} = 0.04 \times 10^{-20} \text{ cm}^2$, and $\Omega_6^{\text{FED}} = 0.08 \times 10^{-20} \text{ cm}^2$.

The $\Omega_\lambda^{\text{FED}}$ calculated values are used, internally in JOYSpectra, to obtain the IET rates. As stated before, a total of 40 transitions for Eu^{3+} and 78 transitions for Tb^{3+} are calculated by the program. These values, for each mechanism, are detailed in [Tables S1 – S4](#) for the Eu^{3+} and in [Tables S5 – S8](#) for the Tb^{3+} compounds.

Table 2 shows the total forward (W^S and W^T) and backward (W_b^S and W_b^T) IET rates, and it is promptly observed that the Eu^{3+} compound exhibits forward rates much larger than backward ones, being ca. 10^8 s^{-1} from the singlet and ca. 10^9 s^{-1} from the triplet state.

Table 2. Forward (W^S and W^T) and backward (W_b^S and W_b^T) IET rates (in s^{-1}) for $[\text{Ln}(\text{tta})_3(\text{H}_2\text{O})_2]$ (Ln: Eu^{3+} and Tb^{3+}).

Compound	W^S	W_b^S	W^T	W_b^T
$[\text{Eu}(\text{tta})_3(\text{H}_2\text{O})_2]$	7.67×10^7	6.50×10^{-1}	7.20×10^8	1.95×10^7
$[\text{Tb}(\text{tta})_3(\text{H}_2\text{O})_2]$	1.71×10^9	4.28×10^9	7.30×10^7	1.35×10^8

On the other hand, for the Tb^{3+} compound, the backward W_b^S and W_b^T rates are larger than the forward ones. This is a direct theoretical observation of the tta^- ligand acting as a good sensitizer for the Eu^{3+} and as a quencher for the Tb^{3+} compound. This effect can also be described in detail by analyzing the Figure 3 diagrams as well as Tables S1 – S8 show the contributions of each energy transfer mechanism involved in the IET rates. Figure 3a shows the ligand S_1 and T_1 relative energies, that can be compared with the Eu^{3+} energy levels, making it evident that the forward paths from both S_1 and T_1 states are energetically favorable, being the backward hindered by the energy mismatch with a negative Δ . A visual qualitative comparison between Figures 3a and 3b makes it clear that the energy mismatches for both S_1 and T_1 states and the Tb^{3+} energy levels, with negative Δ 's for the forward IET pathways [87], are the main reason for the quenching of the luminescence in this compound.

This discussion is quantitatively corroborated by the values of W and W_B depicted in Figure 3. For Eu^{3+} compound, the largest IET rates are the forward $T_1 \rightarrow {}^5D_1$ (pathway 7 in Tables S3), followed by $T_1 \rightarrow {}^5D_0$ (pathway 26 in Tables S3), and $S_1 \rightarrow {}^5G_2$ (pathway 32 in Tables S1), which are depicted as blue arrows in Figures 3a. The most relevant backward pathways, for the Eu^{3+} compound, are $T_1 \leftarrow {}^5D_2$ (pathway 28 in Tables S4), followed by $S_1 \leftarrow {}^5G_2$ (pathway 32 in Tables S2), and $S_1 \leftarrow {}^5G_4$ (pathway 18 in Tables S2), represented by red arrows in Figures 3a. On the other hand, the first two largest IET rates for the Tb^{3+} compound are the backward pathways $S_1 \leftarrow {}^5F_4$ (pathway 67 in Tables S6) and $S_1 \leftarrow {}^5H_4$ (pathway 63 in Tables S6), being the forward $S_1 \rightarrow {}^5F_4$ pathway (67 in Tables S6) the third largest contribution. Additionally, in the Tb^{3+} compound, three of the four main contributions involving the T_1 state are backward IET rates (pathways 8, 47, and 49 in Figure 3b and Table S8), being the sum over them higher than the forward one (pathway 45 in Figure 3b and Table S7).

a)

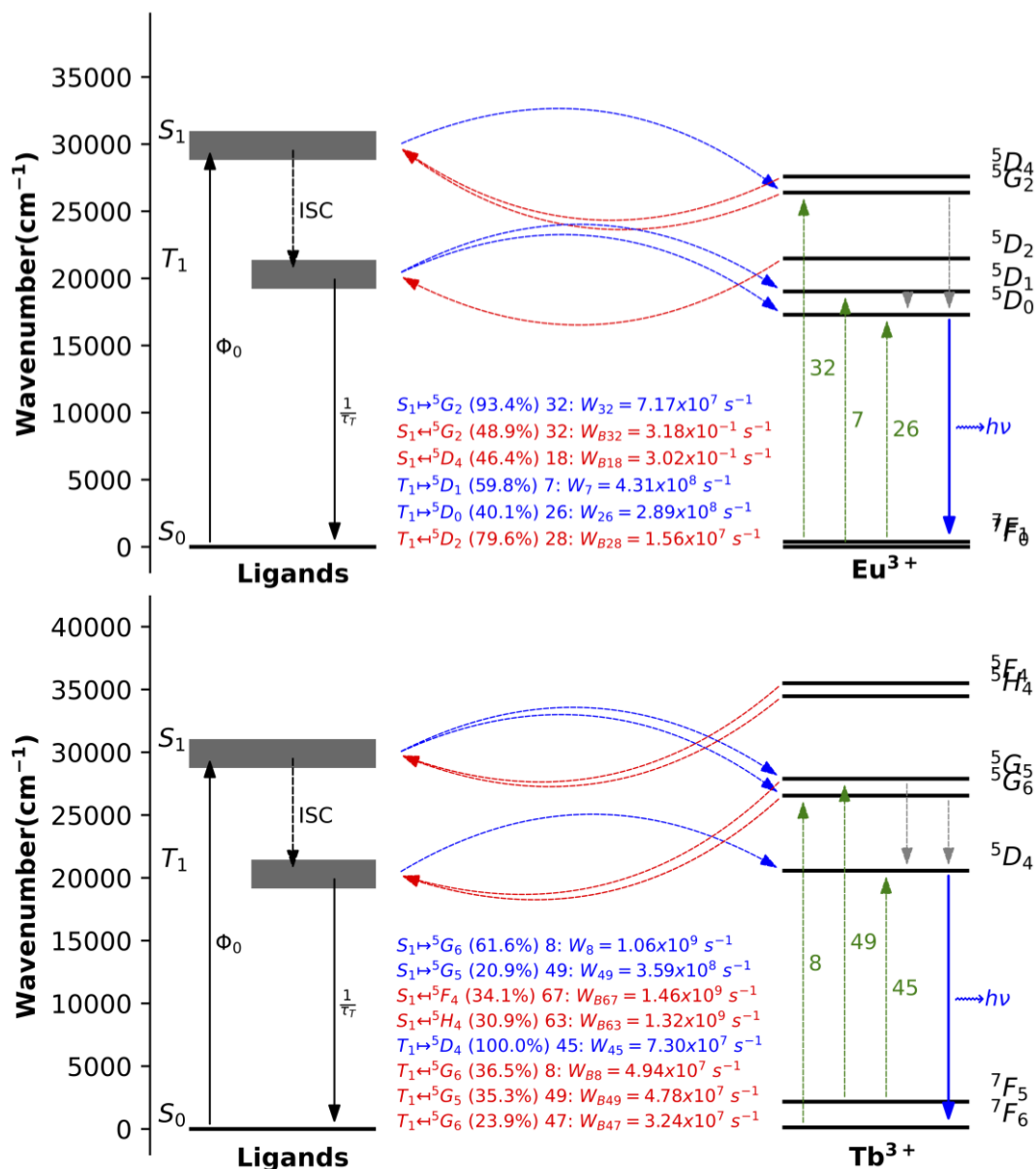


Figure 3. Jablonski-type diagrams for the **a)** [Eu(tta)₃(H₂O)₂] and **b)** [Tb(tta)₃(H₂O)₂] compounds. The blue and red arrows are the forward and backward IET pathways, respectively. Only the pathways representing a minimal contribution of 15% (see Tables S1 – S8) are displayed. Each numbered label corresponds to the pathway listed in Tables S1 – S8. These pictures were generated automatically in the Output viewer module of the JOYSpectra web platform.

It is important to note that these examples were constructed using a straightforward protocol, with the goal of presenting the main functionalities and advantages of the JOYSpectra web platform. Other protocols can be adopted, for instance, the structure and excited states calculated by quantum chemical methods. The quantities g and α' were fitted in the discussed example, but it is possible to use DFT (density functional theory) calculations to estimate these parameters [33,67,70]. The S₁ and T₁ states used in these examples were taken from the experimental data available in the literature, whereas the singlet and triplet excited states at the ligands in the complex could also be calculated by TD-DFT (time-dependent DFT) approaches, which could also provide specific values of R_L for each relevant ligand-based donor states [79]. For more details on theoretical and computational approaches relevant for the use of JOYSpectra see ref. [32].

4. Conclusions

The main features of the luminescence of lanthanide ions based on the extensions of the Judd-Ofelt theory for $4f-4f$ intensities, including FED and DC mechanisms, were successfully implemented in the free-of-charge JOYSpectra web platform. It is expected that this program would be useful to the growing community of experimental and theoretical researchers interested in the photophysical properties of lanthanides. We believe that the program has relevant features that facilitate a better understanding of the chemical and physical information underlying some photophysical properties. It was shown, as a step-by-step example, that the results generated for the $[\text{Eu}(\text{tta})_3(\text{H}_2\text{O})_2]$ and $[\text{Tb}(\text{tta})_3(\text{H}_2\text{O})_2]$ compounds, explained the experimental observation of the tta^- ligand acting as a good sensitizer of Eu^{3+} and as a quencher of the luminescence of the Tb^{3+} compound.

As a perspective, new implementations and functionalities in the JOYSpectra web platform will become promptly available because of its structure and it is online. Thus, the authors do appreciate hearing from the users about bug reports and a wish list of calculable luminescent properties. Indeed, some new developments such as Ln-Ln energy transfer rates calculation, quantum yield and lifetime calculations from numerical solutions of the rate equations, and the effects of nanoparticle plasmons will be available soon.

Acknowledgments

The Brazilian authors are grateful for the financial support from CNPq, CAPES, and FINEP agencies. This work was funded by the Public Call n. 03 *Produtividade em Pesquisa* PROPESQ/PRPG/UFPB project number PVN13305-2020, and PROPESQ/CNPq/UFPB PIN11132-2019. This work was developed within the scope of the project CICECO-Aveiro Institute of Materials, UIDB/50011/2020 and UIDP/50011/2020, financed by Portuguese funds through the FCT/MEC and when appropriate co-financed by FEDER under the PT2020 Partnership Agreement. The Portuguese authors also acknowledge the support of the European Union's Horizon 2020 FET Open program under grant agreement No. 801305 (NanoTBTech). RLL is grateful for the partial financial support under grants: Pronex APQ-0675-1.06/14, INCT-NANOMARCS APQ-0549-1.06/17, APQ-1007-1.06/15, and CNPq-PQ fellowship (Proc. 309177/2018-9).

References

- [1] J.-C.G. Bünzli, Lanthanide light for biology and medical diagnosis, *J. Lumin.* 170 (2016) 866–878. <https://doi.org/10.1016/j.jlumin.2015.07.033>.
- [2] R. Reisfeld, Y. Kalisky, Improved planar solar converter based on uranyl neodymium and holmium glasses, *Nature*. 283 (1980) 281–282. <https://doi.org/10.1038/283281a0>.
- [3] X. Ou, X. Qin, B. Huang, J. Zan, Q. Wu, Z. Hong, L. Xie, H. Bian, Z. Yi, X. Chen, Y. Wu, X. Song, J. Li, Q. Chen, H. Yang, X. Liu, High-resolution X-ray luminescence extension imaging, *Nature*. 590 (2021) 410–415. <https://doi.org/10.1038/s41586-021-03251-6>.
- [4] A.N. Carneiro Neto, O.L. Malta, Glowing nanocrystals enable 3D X-ray imaging, *Nature*. 590 (2021) 396–397. <https://doi.org/10.1038/d41586-021-00350-2>.
- [5] P.P. Lima, S.S. Nobre, R.O. Freire, S.A. Júnior, R.A. Sá Ferreira, U. Pischel, O.L. Malta, L.D. Carlos, Energy transfer mechanisms in organic-inorganic hybrids incorporating europium(III): A quantitative assessment by light emission spectroscopy, *J. Phys. Chem. C*. 111 (2007) 17627–17634. <https://doi.org/10.1021/jp074204e>.
- [6] R.A.S. Ferreira, S.F.H. Correia, A. Monguzzi, X. Liu, F. Meinardi, Spectral converters for photovoltaics – What's ahead, *Mater. Today*. 33 (2020) 105–121.

<https://doi.org/10.1016/j.mattod.2019.10.002>.

- [7] R. Piñol, J. Zeler, C.D.S. Brites, Y. Gu, P. Téllez, A.N. Carneiro Neto, T.E. da Silva, R. Moreno-Loshuertos, P. Fernandez-Silva, A.I. Gallego, L. Martinez-Lostao, A. Martínez, L.D. Carlos, A. Millán, Real-Time Intracellular Temperature Imaging Using Lanthanide-Bearing Polymeric Micelles, *Nano Lett.* 20 (2020) 6466–6472. <https://doi.org/10.1021/acs.nanolett.0c02163>.
- [8] C.D.S. Brites, S. Balabhadra, L.D. Carlos, Lanthanide-Based Thermometers: At the Cutting-Edge of Luminescence Thermometry, *Adv. Opt. Mater.* 7 (2019) 1801239. <https://doi.org/10.1002/adom.201801239>.
- [9] R. Reisfeld, C.K. Jørgensen, *Lasers and Excited States of Rare Earths*, 1st ed., Springer-Verlag Berlin Heidelberg, 1977. <https://doi.org/10.1007/978-3-642-66696-4>.
- [10] M.A. van de Haar, M. Tachikirt, A.C. Berends, M.R. Krames, A. Meijerink, F.T. Rabouw, Saturation Mechanisms in Common LED Phosphors, *ACS Photonics*. (2021) acsphotronics.1c00372. <https://doi.org/10.1021/acsp Photonics.1c00372>.
- [11] G. Blasse, B.C. Grabmaier, *Luminescent Materials*, Springer Berlin Heidelberg, Berlin, Heidelberg, 1994. <https://doi.org/10.1007/978-3-642-79017-1>.
- [12] G. Blasse, K.C. Bleijenberg, R.C. Powell, Luminescence and energy transfer, in: *Struct. Bond. Vol. 42*, Springer-Verlag, Berlin, 1980.
- [13] G. Blasse, Reminiscencies of a quenched luminescence investigatory, *J. Lumin.* 100 (2002) 65–67. [https://doi.org/10.1016/S0022-2313\(02\)00434-9](https://doi.org/10.1016/S0022-2313(02)00434-9).
- [14] G. Blasse, Luminescent materials: is there still news?, *J. Alloys Compd.* 225 (1995) 529–533. [https://doi.org/10.1016/0925-8388\(94\)07096-2](https://doi.org/10.1016/0925-8388(94)07096-2).
- [15] G. Blasse, Luminescence of rare earth ions at the end of the century, *J. Alloys Compd.* 192 (1993) 17–21. [https://doi.org/10.1016/0925-8388\(93\)90172-J](https://doi.org/10.1016/0925-8388(93)90172-J).
- [16] G. Blasse, Rare earth spectroscopy in relation to materials science, *Mater. Chem. Phys.* 31 (1992) 3–6. [https://doi.org/10.1016/0254-0584\(92\)90144-W](https://doi.org/10.1016/0254-0584(92)90144-W).
- [17] B.R. Judd, Optical absorption intensities of rare-earth ions, *Phys. Rev.* 127 (1962) 750–761. <https://doi.org/10.1103/PhysRev.127.750>.
- [18] G.S. Ofelt, Intensities of Crystal Spectra of Rare-Earth Ions, *J. Chem. Phys.* 37 (1962) 511–520. <https://doi.org/10.1063/1.1701366>.
- [19] J. Sytsma, G.F. Imbusch, G. Blasse, The spectroscopy of Gd^{3+} in yttriumoxychloride: Judd–Ofelt parameters from emission data, *J. Chem. Phys.* 91 (1989) 1456–1461. <https://doi.org/10.1063/1.457106>.
- [20] R. Reisfeld, Spectra and energy transfer of rare earths in inorganic glasses, in: *Rare Earths. Struct. Bond. Vol 13*, Berlin, Heidelberg, 1973: pp. 53–98. https://doi.org/10.1007/3-540-06125-8_2.
- [21] G.S. Ofelt, Intensities of crystal spectra of rare-earth ions, *J. Chem. Phys.* 37 (1962) 511–520. <https://doi.org/10.1063/1.1701366>.
- [22] R. Reisfeld, C.K. Jørgensen, Luminescent Solar Concentrators for Energy Conversion, *Struct. Bond.* 49 (1982) 1–36. <https://doi.org/10.1007/BFb0111291>.

- [23] P.A.M. Berdowski, G. Blasse, Non-radiative relaxation of the $\text{Eu}^{3+} \ ^5\text{D}_1$ level in NaGdTiO_4 , *Chem. Phys. Lett.* 107 (1984) 351–354. [https://doi.org/10.1016/0009-2614\(84\)85143-X](https://doi.org/10.1016/0009-2614(84)85143-X).
- [24] B.G. Wybourne, Structure of f^n Configurations. II. f^5 and f^9 Configurations, *J. Chem. Phys.* 36 (1962) 2301–2311. <https://doi.org/10.1063/1.1732880>.
- [25] W.T. Carnall, P.R. Fields, K. Rajnak, Electronic Energy Levels in the Trivalent Lanthanide Aquo Ions. I. Pr^{3+} , Nd^{3+} , Pm^{3+} , Sm^{3+} , Dy^{3+} , Ho^{3+} , Er^{3+} , and Tm^{3+} , *J. Chem. Phys.* 49 (1968) 4424–4442. <https://doi.org/10.1063/1.1669893>.
- [26] W.T. Carnall, P.R. Fields, K. Rajnak, Electronic Energy Levels of the Trivalent Lanthanide Aquo Ions. III. Tb^{3+} , *J. Chem. Phys.* 49 (1968) 4447–4449. <https://doi.org/10.1063/1.1669895>.
- [27] G.H. Dieke, H.M. Crosswhite, The Spectra of the Doubly and Triply Ionized Rare Earths, *Appl. Opt.* 2 (1963) 675. <https://doi.org/10.1364/AO.2.000675>.
- [28] D.L. Dexter, A Theory of Sensitized Luminescence in Solids, *J. Chem. Phys.* 21 (1953) 836–850. <https://doi.org/10.1063/1.1699044>.
- [29] D.L. Dexter, J.H. Schulman, Theory of Concentration Quenching in Inorganic Phosphors, *J. Chem. Phys.* 22 (1954) 1063–1070. <https://doi.org/10.1063/1.1740265>.
- [30] T. Kushida, Energy Transfer and Cooperative Optical Transitions in Rare-Earth Doped Inorganic Materials. I. Transition Probability Calculation, *J. Phys. Soc. Japan.* 34 (1973) 1318–1326. <https://doi.org/10.1143/JPSJ.34.1318>.
- [31] M.P. Hehlen, M.G. Brik, K.W. Krämer, 50th anniversary of the Judd-Ofelt theory: An experimentalist's view of the formalism and its application, *J. Lumin.* 136 (2013) 221–239. <https://doi.org/10.1016/j.jlumin.2012.10.035>.
- [32] A.N. Carneiro Neto, E.E.S. Teotonio, G.F. de Sá, H.F. Brito, J. Legendziewicz, L.D. Carlos, M.C.F.C. Felinto, P. Gawryszewska, R.T. Moura Jr., R.L. Longo, W.M. Faustino, O.L. Malta, Modeling intramolecular energy transfer in lanthanide chelates: A critical review and recent advances, in: J.-C.G. Bünzli, V.K. Pecharsky (Eds.), *Handb. Phys. Chem. Rare Earths*, Vol. 56, Elsevier, 2019: pp. 55–162. <https://doi.org/10.1016/bs.hpre.2019.08.001>.
- [33] R.T. Moura, A.N. Carneiro Neto, R.L. Longo, O.L. Malta, On the calculation and interpretation of covalency in the intensity parameters of $4f-4f$ transitions in Eu^{3+} complexes based on the chemical bond overlap polarizability, *J. Lumin.* 170 (2016) 420–430. <https://doi.org/10.1016/j.jlumin.2015.08.016>.
- [34] O.L. Malta, A simple overlap model in lanthanide crystal-field theory, *Chem. Phys. Lett.* 87 (1982) 27–29. [https://doi.org/10.1016/0009-2614\(82\)83546-X](https://doi.org/10.1016/0009-2614(82)83546-X).
- [35] O.L. Malta, Theoretical crystal-field parameters for the $\text{YOCl}:\text{Eu}^{3+}$ system. A simple overlap model, *Chem. Phys. Lett.* 88 (1982) 353–356. [https://doi.org/10.1016/0009-2614\(82\)87103-0](https://doi.org/10.1016/0009-2614(82)87103-0).
- [36] M. Suta, F. Cimpoesu, W. Umland, The angular overlap model of ligand field theory for f elements: An intuitive approach building bridges between theory and experiment, *Coord. Chem. Rev.* 441 (2021) 213981. <https://doi.org/10.1016/j.ccr.2021.213981>.
- [37] W. Umland, On the ligand-field potential for f electrons in the angular overlap model, *Chem. Phys.* 14 (1976) 393–401. [https://doi.org/10.1016/0301-0104\(76\)80136-X](https://doi.org/10.1016/0301-0104(76)80136-X).
- [38] B.Z. Malkin, Z.I. Ivanenko, I.B. Aizenberg, Crystal field in uniaxially compressed $\text{MeF}_2:\text{Ln}$ crystals,

Sov. Phys. Solid State. 12 (1970) 1491–1496.

- [39] L.K. Aminov, B.Z. Malkin, M.A. Teplov, Magnetic properties of nonmetallic lanthanide compounds, in: K.A. Gschneidner Jr., L. Eyring (Eds.), *Handb. Phys. Chem. Rare Earths*, Elsevier, 1996: pp. 295–506. [https://doi.org/10.1016/S0168-1273\(96\)22007-0](https://doi.org/10.1016/S0168-1273(96)22007-0).
- [40] C.A. Morrison, G.F. de Sá, R.P. Leavitt, Self-induced multipole contribution to the single-electron crystal field, *J. Chem. Phys.* 76 (1982) 3899–3904. <https://doi.org/10.1063/1.443477>.
- [41] D. Garcia, M. Faucher, Crystal field parameters in rare earth compounds: A mixed "covalencelectrostatic model", *J. Chem. Phys.* 82 (1985) 5554–5564. <https://doi.org/10.1063/1.448590>.
- [42] S.I. Weissman, Intramolecular energy transfer the fluorescence of complexes of Europium, *J. Chem. Phys.* 10 (1942) 214–217. <https://doi.org/10.1063/1.1723709>.
- [43] N. Yamada, S. Shionoya, T. Kushida, Phonon-Assisted Energy Transfer between Trivalent Rare Earth Ions, *J. Phys. Soc. Japan.* 32 (1972) 1577–1586. <https://doi.org/10.1143/JPSJ.32.1577>.
- [44] A.N. Carneiro Neto, R.T. Moura, A. Shyichuk, V. Paterlini, F. Piccinelli, M. Bettinelli, O.L. Malta, Theoretical and Experimental Investigation of the $Tb^{3+} \rightarrow Eu^{3+}$ Energy Transfer Mechanisms in Cubic $A_3Tb_{0.90}Eu_{0.10}(PO_4)_3$ ($A = Sr, Ba$) Materials, *J. Phys. Chem. C.* 124 (2020) 10105–10116. <https://doi.org/10.1021/acs.jpcc.0c00759>.
- [45] V. Trannoy, A.N. Carneiro Neto, C.D.S. Brites, L.D. Carlos, H. Serier-Brault, Engineering of Mixed Eu^{3+}/Tb^{3+} Metal-Organic Frameworks Luminescent Thermometers with Tunable Sensitivity, *Adv. Opt. Mater.* 2001938 (2021) 2001938. <https://doi.org/10.1002/adom.202001938>.
- [46] M.A. Hernández-Rodríguez, C.D.S. Brites, G. Antorrena, R. Piñol, R. Cases, L. Pérez-García, M. Rodrigues, J.A. Plaza, N. Torras, I. Díez, A. Millán, L.D. Carlos, Lanthanide Luminescence to Mimic Molecular Logic and Computing through Physical Inputs, *Adv. Opt. Mater.* 8 (2020) 2000312. <https://doi.org/10.1002/adom.202000312>.
- [47] C.G. Gameiro, E.F. da Silva Jr., S. Alves Jr., G. de Sá, P. Santa-Cruz, Lanthanide complexes dispersed in enamel: a promising new material for photonic devices, *J. Alloys Compd.* 323–324 (2001) 820–823. [https://doi.org/10.1016/S0925-8388\(01\)01152-5](https://doi.org/10.1016/S0925-8388(01)01152-5).
- [48] C.D.S. Brites, A. Millán, L.D. Carlos, Lanthanides in Luminescent Thermometry, in: J.-C.G. Bünzli, V.K. Pecharsky (Eds.), *Handb. Phys. Chem. Rare Earths*, Vol. 49, Elsevier, 2016: pp. 339–427. <https://doi.org/10.1016/bs.hpcr.2016.03.005>.
- [49] L. Zhao, J. Mao, B. Jiang, X. Wei, M. Yin, Y. Chen, A new yellow long persistent luminescence phosphor $Ca_2Al_2SiO_7:Eu^{2+},Tm^{3+}$ found by co-doping Ln^{3+} ($Ln = Ce, Pr, Nd, Sm, Gd, Tb, Dy, Ho, Er, Tm, Yb, Lu$) with Eu^{2+} in Ca_2A , *J. Lumin.* 206 (2019) 6–10. <https://doi.org/10.1016/j.jlumin.2018.10.038>.
- [50] T. Aitasalo, J. Hölsä, J.-C. Krupa, M. Lastusaari, J. Niittykoski, Persistent Luminescence Materials, in: *Phys. Laser Cryst.*, Springer Netherlands, Dordrecht, 2003: pp. 35–50. https://doi.org/10.1007/978-94-010-0031-4_3.
- [51] A. Lecointre, A. Bessière, A.J.J. Bos, P. Dorenbos, B. Viana, S. Jacquart, Designing a Red Persistent Luminescence Phosphor: The Example of $YPO_4:Pr^{3+},Ln^{3+}$ ($Ln = Nd, Er, Ho, Dy$), *J. Phys. Chem. C.* 115 (2011) 4217–4227. <https://doi.org/10.1021/jp108038v>.
- [52] H.F. Brito, O.M.L. Malta, M.C.F.C. Felinto, E.E.S. Teotonio, Luminescence phenomena involving

metal enolates, in: J. Zabicky (Ed.), *Chem. Met. Enolates*, Wiley-VCH Verlag GmbH, Weinheim, Germany, 2009: pp. 131–177. <https://doi.org/10.1002/9783527615858>.

- [53] D.N. Woodruff, R.E.P. Winpenny, R.A. Layfield, *Lanthanide Single-Molecule Magnets*, *Chem. Rev.* 113 (2013) 5110–5148. <https://doi.org/10.1021/cr400018q>.
- [54] J.D.L. Dutra, T.D. Bispo, R.O. Freire, LUMPAC lanthanide luminescence software: Efficient and user friendly, *J. Comput. Chem.* 35 (2014) 772–775. <https://doi.org/10.1002/jcc.23542>.
- [55] R.O. Freire, G.B. Rocha, A.M. Simas, Sparkle model for the calculation of lanthanide complexes: AM1 parameters for Eu(III), Gd(III), and Tb(III), *Inorg. Chem.* 44 (2005) 3299–3310. <https://doi.org/10.1021/ic048530+>.
- [56] J.J.P. Stewart, MOPAC2016, (2016). <http://openmopac.net>.
- [57] S.F. Mason, R.D. Peacock, B. Stewart, Ligand-polarization contributions to the intensity of hypersensitive trivalent lanthanide transitions, *Mol. Phys.* 30 (1975) 1829–1841. <https://doi.org/10.1080/00268977500103321>.
- [58] A. Ćirić, S. Stojadinović, M. Sekulić, M.D. Dramićanin, JOES: An application software for Judd-Ofelt analysis from Eu³⁺ emission spectra, *J. Lumin.* 205 (2019) 351–356. <https://doi.org/10.1016/j.jlumin.2018.09.048>.
- [59] Y.H. Pham, V.A. Trush, A.N. Carneiro Neto, M. Korabik, J. Sokolnicki, M. Weselski, O.L. Malta, V.M. Amirkhanov, P. Gawryszewska, Lanthanide complexes with N -phosphorylated carboxamide as UV converters with excellent emission quantum yield and single-ion magnet behavior, *J. Mater. Chem. C* 8 (2020) 9993–10009. <https://doi.org/10.1039/D0TC01445A>.
- [60] M. Hehlen, A.N. Carneiro Neto, Personal communication, (2020).
- [61] S. Sato, M. Wada, Relations between Intramolecular Energy Transfer Efficiencies and Triplet State Energies in Rare Earth β -diketone Chelates, *Bull. Chem. Soc. Jpn.* 43 (1970) 1955–1962. <https://doi.org/10.1246/bcsj.43.1955>.
- [62] A.S. Souza, L.A. Nunes, M.C.F.C. Felinto, H.F. Brito, O.L. Malta, On the quenching of trivalent terbium luminescence by ligand low lying triplet state energy and the role of the ⁷F₅ level: The [Tb(tta)₃(H₂O)₂] case, *J. Lumin.* 167 (2015) 167–171. <https://doi.org/10.1016/j.jlumin.2015.06.020>.
- [63] E.E.S. Teotonio, H.F. Brito, G.F. de Sá, M.C.F.C. Felinto, R.H.A. Santos, R.M. Fuquen, I.F. Costa, A.R. Kennedy, D. Gilmore, W.M. Faustino, Structure and luminescent investigation of the Ln(III)– β -diketonate complexes containing tertiary amides, *Polyhedron*. 38 (2012) 58–67. <https://doi.org/10.1016/j.poly.2012.02.010>.
- [64] Jmol: an open-source Java viewer for chemical structures in 3D, (2019). <http://www.jmol.org/>.
- [65] M.J. Frisch, G.W. Trucks, H.B. Schlegel, G.E. Scuseria, M.A. Robb, J.R. Cheeseman, G. Scalmani, V. Barone, G.A. Petersson, H. Nakatsuji, X. Li, M. Caricato, A. V. Marenich, J. Bloino, B.G. Janesko, R. Gomperts, B. Mennucci, H.P. Hratchian, J. V. Ortiz, A.F. Izmaylov, J.L. Sonnenberg, D. Williams-Young, F. Ding, F. Lipparini, F. Egidi, J. Goings, B. Peng, A. Petrone, T. Henderson, D. Ranasinghe, V.G. Zakrzewski, J. Gao, N. Rega, G. Zheng, W. Liang, M. Hada, M. Ehara, K. Toyota, R. Fukuda, J. Hasegawa, M. Ishida, T. Nakajima, Y. Honda, O. Kitao, H. Nakai, T. Vreven, K. Throssell, J.A.J. Montgomery, J.E. Peralta, F. Ogliaro, M.J. Bearpark, J.J. Heyd, E.N. Brothers, K.N. Kudin, V.N. Staroverov, T.A. Keith, R. Kobayashi, J. Normand, K. Raghavachari, A.P. Rendell, J.C. Burant, S.S. Iyengar, J. Tomasi, M. Cossi, J.M. Millam, M. Klene, C. Adamo, R.

- Cammi, J.W. Ochterski, R.L. Martin, K. Morokuma, O. Farkas, J.B. Foresman, D.J. Fox, Gaussian 16, Revision C.01, (2016).
- [66] F. Neese, Software update: the ORCA program system, version 4.0, WIREs Comput. Mol. Sci. 8 (2018). <https://doi.org/10.1002/wcms.1327>.
- [67] A.N. Carneiro Neto, R.T. Moura, E.C. Aguiar, C. V Santos, M.A.F.L.B. de Medeiros, Theoretical study of geometric and spectroscopic properties of Eu(III) complexes with Ruhemann's Purple ligands, J. Lumin. 201 (2018) 451–459. <https://doi.org/10.1016/j.jlumin.2018.05.014>.
- [68] A. Shyichuk, R.T. Moura, A.N.C. Neto, M. Runowski, M.S. Zarad, A. Szczeszak, S. Lis, O.L. Malta, Effects of Dopant Addition on Lattice and Luminescence Intensity Parameters of Eu(III)-Doped Lanthanum Orthovanadate, J. Phys. Chem. C. 120 (2016) 28497–28508. <https://doi.org/10.1021/acs.jpcc.6b10778>.
- [69] G.B.V. Lima, J.C. Bueno, A.F. da Silva, A.N. Carneiro Neto, R.T. Moura, E.E.S. Teotonio, O.L. Malta, W.M. Faustino, Novel trivalent europium β -diketonate complexes with N-(pyridine-2-yl)amides and N-(pyrimidine-2-yl)amides as ancillary ligands: Photophysical properties and theoretical structural modeling, J. Lumin. 219 (2020) 116884. <https://doi.org/10.1016/j.jlumin.2019.116884>.
- [70] P.R.S. Santos, D.K.S. Pereira, I.F. Costa, I.F. Silva, H.F. Brito, W.M. Faustino, A.N. Carneiro Neto, R.T. Moura, M.H. Araujo, R. Diniz, O.L. Malta, E.E.S. Teotonio, Experimental and theoretical investigations of the $[\text{Ln}(\beta\text{-dik})(\text{NO}_3)_2(\text{phen})_2]\cdot\text{H}_2\text{O}$ luminescent complexes, J. Lumin. 226 (2020) 117455. <https://doi.org/10.1016/j.jlumin.2020.117455>.
- [71] T. Grzyb, A. Szczeszak, A. Shyichuk, R.T. Moura, A.N.C. Neto, N. Andrzejewska, O.L. Malta, S. Lis, Comparative studies of structure, spectroscopic properties and intensity parameters of tetragonal rare earth vanadate nanophosphors doped with Eu(III), J. Alloys Compd. 741 (2018) 459–472. <https://doi.org/10.1016/j.jallcom.2018.01.095>.
- [72] A.N. Carneiro Neto, R.T. Moura, O.L. Malta, On the mechanisms of non-radiative energy transfer between lanthanide ions: centrosymmetric systems, J. Lumin. 210 (2019) 342–347. <https://doi.org/10.1016/j.jlumin.2019.02.049>.
- [73] L. Smentek, A. Ke dziorski, Efficiency of the energy transfer in lanthanide-organic chelates; spectral overlap integral, J. Lumin. 130 (2010) 1154–1159. <https://doi.org/10.1016/j.jlumin.2010.02.013>.
- [74] R.T. Moura, J.A. Oliveira, I.A. Santos, E.M. Lima, L.D. Carlos, E.C. Aguiar, A.N.C. Neto, Theoretical Evidence of the Singlet Predominance in the Intramolecular Energy Transfer in Ruhemann's Purple Tb(III) Complexes, Adv. Theory Simulations. 4 (2021) 2000304. <https://doi.org/10.1002/adts.202000304>.
- [75] O.L. Malta, Energy transfer between molecules and small metallic particles, Phys. Lett. A. 114 (1986) 195–197. [https://doi.org/10.1016/0375-9601\(86\)90204-5](https://doi.org/10.1016/0375-9601(86)90204-5).
- [76] W.J.C. Grant, Role of Rate Equations in the Theory of Luminescent Energy Transfer, Phys. Rev. B. 4 (1971) 648–663. <https://doi.org/10.1103/PhysRevB.4.648>.
- [77] K.-L. Wong, J.-C.G. Bünzli, P.A. Tanner, Quantum yield and brightness, J. Lumin. 224 (2020) 117256. <https://doi.org/10.1016/j.jlumin.2020.117256>.
- [78] E.S. Teixeira, B.B. Neto, P.M.C. de Oliveira, R.L. Longo, Chemometric analysis of the luminescence quantum yields in lanthanide ion complexes, J. Lumin. 170 (2016) 602–613.

<https://doi.org/10.1016/j.jlumin.2014.10.033>.

- [79] E. Kasprzycka, A.N. Carneiro Neto, V.A. Trush, L. Jerzykiewicz, V.M. Amirkhanov, O.L. Malta, J. Legendziewicz, P. Gawryszewska, How minor structural changes generate major consequences in photophysical properties of RE coordination compounds; resonance effect, LMCT state, *J. Rare Earths*. 38 (2020) 552–563. <https://doi.org/10.1016/j.jre.2020.02.001>.
- [80] R.A.S. Ferreira, M. Nolasco, A.C. Roma, R.L. Longo, O.L. Malta, L.D. Carlos, Dependence of the Lifetime upon the Excitation Energy and Intramolecular Energy Transfer Rates: The 5D₀ Eu^{III} Emission Case, *Chem. - A Eur. J.* 18 (2012) 12130–12139. <https://doi.org/10.1002/chem.201201736>.
- [81] F. Caixeta, A. Bastos, A. Botas, L. Rosa, V. Souza, F. Borges, A. Carneiro Neto, A. Ferrier, P. Goldner, L. Carlos, R. Gonçalves, R. Ferreira, High-Quantum-Yield Upconverting Er³⁺/Yb³⁺-Organic–Inorganic Hybrid Dual Coatings for Real-Time Temperature Sensing and Photothermal Conversion, *J. Phys. Chem. C*. 124 (2020) 19892–19903. <https://doi.org/10.1021/acs.jpcc.0c03874>.
- [82] X. Qin, A.N. Carneiro Neto, R.L. Longo, Y. Wu, O.L. Malta, X. Liu, Surface Plasmon-Photon Coupling in Lanthanide-Doped Nanoparticles, *J. Phys. Chem. Lett.* 12 (2021) 1520–1541. <https://doi.org/10.1021/acs.jpcclett.0c03613>.
- [83] A.N. Carneiro Neto, M.A. Couto dos Santos, O.L. Malta, R. Reisfeld, Effects of Spherical Metallic Nanoparticle Plasmon on 4f-4f Luminescence: A Theoretical Approach, in: L.R.P. Kassab, C.B. de Araujo (Eds.), *Met. Nanostructures Photonics*, 1st ed., Elsevier, 2019: pp. 19–36. <https://doi.org/10.1016/B978-0-08-102378-5.00002-7>.
- [84] V. Vallet, A. Fischer, Z. Szabó, I. Grenthe, The structure and bonding of Y, Eu, U, Am and Cm complexes as studied by quantum chemical methods and X-ray crystallography, *Dalt. Trans.* 39 (2010) 7666. <https://doi.org/10.1039/b926508b>.
- [85] L.E. do N. Aquino, G.A. Barbosa, J. de L. Ramos, S. O. K. Giese, F.S. Santana, D.L. Hughes, G.G. Nunes, L. Fu, M. Fang, G. Poneti, A.N. Carneiro Neto, R.T. Moura, R.A.S. Ferreira, L.D. Carlos, A.G. Macedo, J.F. Soares, Seven-Coordinate Tb³⁺ Complexes with 90% Quantum Yields: High-Performance Examples of Combined Singlet- and Triplet-to-Tb³⁺ Energy-Transfer Pathways, *Inorg. Chem.* 60 (2021) 892–907. <https://doi.org/10.1021/acs.inorgchem.0c03020>.
- [86] G.F. de Sá, O.L. Malta, C. de Mello Donegá, A.M. Simas, R.L. Longo, P.A. Santa-Cruz, E.F. da Silva, Spectroscopic properties and design of highly luminescent lanthanide coordination complexes, *Coord. Chem. Rev.* 196 (2000) 165–195. [https://doi.org/10.1016/S0010-8545\(99\)00054-5](https://doi.org/10.1016/S0010-8545(99)00054-5).
- [87] M. Latva, H. Takalo, V.-M. Mikkala, C. Matesescu, J.C. Rodríguez-Ubis, J. Kankare, Correlation between the lowest triplet state energy level of the ligand and lanthanide(III) luminescence quantum yield, *J. Lumin.* 75 (1997) 149–169. [https://doi.org/10.1016/S0022-2313\(97\)00113-0](https://doi.org/10.1016/S0022-2313(97)00113-0).